Bachelor thesis

Numerical simulations of Rabi-type oscillations in an N-level-system

by

Christina Madl

supervised by

Assoz. Prof. Dipl.-Ing. Dr. Peter Puschnig

University of Graz, Austria

Institute of Physics

October 7, 2023

Abstract

In this thesis, a quantum mechanical system is considered which is described by N discrete energy levels. Starting with a system in the ground state and coupling to an external electromagnetical field with a specific frequency can result in the occupation of higher energy levels. If the external field is periodic in time the occupation of the excited states is also excpected to be periodic, leading to what is called a Rabi oscillation. The interaction between the system and the driving field can be described using the Schrödinger equation with the minimal coupling Hamiltonian. The time-dependent Schrödinger equation is solved by using an ansatz for the wave function consisting of a linear superposition of the N states of the unperturbed system. The absolute squares of their coefficients then represent the occupation of the corresponding level. Finally, this ansatz leads to a system of first order differential equations which are difficult to solve analytically. Therefore, the focus of this thesis is to solve these differential equations numerically using the Runge-Kutta-method of 4th order.

Contents

1 Introduction

1.1 Units

In this work the atomic unit system is used. This implies in all equations $\hbar = m_e = \frac{e^2}{4\pi\epsilon_0} = 1$ a.u. (atomic unit) if not stated otherwise.

1.2 Rabi-Oscillations

Consider a quantum mechanical system with N energy levels. As energy levels in quantum mechanics are discrete, in the case of a transition from an energy level E_k to an energy level E_n the difference of the energies $\Delta E = E_n - E_k$ is absorbed/released. A positive value of ΔE describes a transition of a lower energy level to a higher one. This means the system has to absorb this energy to enable the transition. A negative value of ΔE describes a transition from a level with higher energy to a level with lower energy. In this case the system releases energy to the surroundings.

So, assuming the system is in the ground state, an energy supply is needed to enable the occupation of higher states. To supply this energy, we consider an external, periodic driving field of the form $E(t) = E_0 \cdot \cos(\omega t)$ [1]. If an excited state is occupied, the system does not stay at this higher energy level for long. When it falls back to a lower level, the energy ΔE is given back to the external field. This results in an oscillation of the system between energy levels which is referred to as a Rabi-Oscillation.

The condition for the Rabi-Oscillation is that the energy provided by the driving field is close to the energy difference ΔE between energy levels E_k and E_n. In other words, the frequency ω of the driving field has to be close to the resonant frequency

$$\omega_{nk} = E_n - E_k. \tag{1}$$

As a measure for the difference between the resonant frequency and the driving field frequency, the detuning δ is introduced:

$$\delta_{nk} := \omega - \omega_{nk}, \tag{2}$$

where it is commonly assumed that $\delta_{nk} \ll \omega + \omega_{nk}$ [8].

2 Quantum-mechanical description of Rabi-oscillations

The derivation in this chapter largely follows Ref. [1]. However, in this work a N-level-system instead of a two-level-system is considered. To describe an unperturbed N-level-system, the time-independent Schrödinger equation

$$\hat{H}_0 \left|\varphi_n\right\rangle = E_n \left|\varphi_n\right\rangle \tag{3}$$

is used, where the $|\varphi_n\rangle$ are the states associated with the energy levels E_n, and $\hat{H}_0$ is the unperturbed Hamiltonian. To represent the driving field the perturbation Hamiltonian $\hat{H}'$ is added, which results in the minimal coupling Hamiltonian [4]

$$\hat{H} = \hat{H}_0 + \hat{H}' = \frac{1}{2m}\left(\hat{\mathbf{p}} - q\hat{\mathbf{A}}(\mathbf{r},t)\right)^2 + q\hat{\Phi}(\mathbf{r},t). \tag{4}$$

Here, $\hat{\mathbf{p}}$ is the momentum, q is the charge, $\hat{\mathbf{A}}(\mathbf{r},t)$ the vector potential of the electromagnetic field and $\hat{\Phi}(\mathbf{r},t)$ its scalar potential.

By using the dipole approximation, where we assume that the wavelength of the electromagnetic field is a lot bigger than an atom, the spatial component of the vector potential can be neglected: $\hat{\mathbf{A}}(\mathbf{r},t) \approx \hat{\mathbf{A}}(t)$. Furthermore, the Göppert-Mayer-gauge [6] is introduced. This gauge uses the transformation

$$\hat{\chi}(t) = -\hat{\mathbf{x}}\hat{\mathbf{A}}'(t), \tag{5}$$

where $\hat{\mathbf{x}}$ represents the position operator. The Göppert-Mayer-gauge results in

$$\hat{\mathbf{A}}(t) = \hat{\mathbf{A}}'(t) + \nabla\hat{\chi}(t) = 0 \tag{6}$$

$$q\hat{\Phi}(\mathbf{r},t) = \hat{\Phi}'(\mathbf{r},t) - \partial_t\hat{\chi}(t) = q\hat{\mathbf{x}}\hat{\mathbf{E}}(t). \tag{7}$$

Finally, after using the dipole approximation and the Göppert-Mayer-gauge, the Hamiltonian of the system is given by

$$\hat{H} = \frac{1}{2}\ \hat{\mathbf{p}}^2 + q\hat{\mathbf{x}}\ \hat{\mathbf{E}}_0\ \cos(\omega t). \tag{8}$$

Next, we assume that the wave function describing the perturbed system is a superposition of the wave functions of the unperturbed system

$$\left|\psi(t)\right\rangle = \sum_{n=1}^{N} c_n(t)\ e^{-iE_n t}\left|\varphi_n\right\rangle. \tag{9}$$

In this equation, the phase factor $e^{-iE_n t}$ arises from the time evolution of the unperturbed wave functions.

Inserting this ansatz into the time-dependent Schrödinger equation

$$i\ \partial_t \left|\psi(t)\right\rangle = \hat{H}\left|\psi(t)\right\rangle \tag{10}$$

results in

$$\sum_{n=1}^{N} i\ \dot{c}_n(t)\ e^{-iE_n t}\left|\varphi_n\right\rangle = \sum_{n=1}^{N} c_n(t)\ e^{-iE_n t}\hat{H}'\left|\varphi_n\right\rangle, \tag{11}$$

where $\dot{c}_n(t)$ denotes the time derivative of the coefficients. Multiplying Eq. 11 from the left by $\langle\varphi_k|$ with k = 1, 2, ..., N leads to

$$\dot{c}_k(t) = -i\sum_{n=1}^{N} c_n(t)\ e^{-i\omega_{nk}t}H'_{kn} \tag{12}$$

with the matrix elements of the Hamiltonian defined as

$$H'_{kn} = \left\langle\varphi_k\right|\hat{H}'\left|\varphi_n\right\rangle. \tag{13}$$

As suggested by Eq. 8, the perturbation Hamiltonian has the form

$$\hat{H}' = q\hat{\mathbf{x}}\ \mathbf{E}_0\ \cos(\omega t). \tag{14}$$

Substituting this Hamiltonian into Eq. 13 yields

$$\begin{aligned} H_{kn} &= q\ \left\langle\varphi_k\right|\hat{\mathbf{x}}\left|\varphi_n\right\rangle \mathbf{E}_0\cos(\omega t) \\ &= q\ \mathbf{x}_{kn}\mathbf{E}_0\cos(\omega t) \\ &= \mathbf{d}_{kn}\mathbf{E}_0\cos(\omega t) \\ &= \Omega_{kn}\cos(\omega t) \\ &= H'_{nk}. \end{aligned} \tag{15}$$

In this equation the transition dipole moment $\mathbf{d}_{kn}$ with the property $\mathbf{d}_{kn} = \mathbf{d}_{nk}$ and $\mathbf{d}_{nn}$ = 0 [3] was introduced. Furthermore, the Rabi-frequency

$$\Omega_{kn} := \mathbf{d}_{kn}\mathbf{E}_0 \tag{16}$$

was defined. This frequency describes how fast the system oscillates between two energy levels E_k and E_n. It is proportional to the amplitude of the electromagnetic field and the interaction between the system and the field.

Finally, substituting the matrix elements from Eq. 13 into Eq. 12 results in

$$\dot{c}_k(t) = -i\ \sum_{n=1}^{N} c_n(t)\ \frac{\Omega_{nk}}{2}\ (e^{i(\omega-\omega_{nk})t} + e^{-i(\omega+\omega_{nk})t}). \tag{17}$$

Note that here excluding $n = k$ from the sum happens automatically as a result of the definition of the dipole moment $d_{nn} = 0$ and therefore $\Omega_{nn} = 0$. Eq. 17 now decribes a system of homogenous, linear differential equations for the coefficients $c_k(t)$. Solving these differential equations will be the central focus of this work, as the absolute square of the coefficients $|c_k(t)|^2$ represents the probability of the system occupying a state with energy E_k.

The second quantity that is of interest is the expectation value of the dipole moment

$$\mathbf{d} = \langle\psi|\,\hat{\mathbf{d}}\,|\psi\rangle = \sum_{n,k=1}^{N} c_n^*(t)\; c_k(t)\; e^{i\omega_{nk}t}\; \mathbf{d}_{nk}. \tag{18}$$

From now on we assume the driving field $\mathbf{E}(t)$ is polarized in z-direction which, according to Eq. 16, leaves only the z-component of $\mathbf{d}$ of concern. With that in mind, d_z will be referred to simply as d and Eq. 18 can be rewritten as

$$d(t) = \sum_{n,k=1}^{N} c_n^*(t)\; c_k(t)\; e^{i\omega_{nk}t}\; d_{nk}. \tag{19}$$

3 Numerical solution

The objective of this chapter is to solve Eq. 17 numerically and then compute the dipole moment from Eq. 19. Firstly, Eq. 17 will be treated as an initial value problem with the initial values

$$c_k(0) = \begin{cases} 1 & \text{if } k = 1 \\ 0 & \text{otherwise.} \end{cases} \tag{20}$$

This means the system starts with a fully occupied ground state and no other state is populated. To solve this initial value problem, a Runge-Kutta method of 4th order will be used and therefore briefly be explained here. The differential equations in this case have the form

$$\dot{\mathbf{y}} = \mathbf{f}(t, \mathbf{y}), \tag{21}$$

where $\mathbf{y}$ and $\dot{\mathbf{y}}$ are vectors with the components y_k and $\dot{y}_k$ with k = 1, 2,..., N respectively. The time is discretised into equally spaced intervals with a width Δt. The method then starts with the initial values of $\mathbf{y}(0) = \mathbf{y}_0$. Then, for each discrete timestep t_n four approximate values $\mathbf{k}_1, \mathbf{k}_2, \mathbf{k}_3$ and $\mathbf{k}_4$ for the derivative vector $\dot{\mathbf{y}}$ are calculated in the following way with $\mathbf{y}_n := \mathbf{y}(t_n)$ [7]:

$$\mathbf{k}_1 = \mathbf{f}(t_n, \mathbf{y}_n) \tag{22}$$

$$\mathbf{k}_2 = \mathbf{f}\left(t_n + \frac{\Delta t}{2}, \mathbf{y}_n + \frac{\Delta t}{2}\mathbf{k}_1\right) \tag{23}$$

$$\mathbf{k}_3 = \mathbf{f}\left(t_n + \frac{\Delta t}{2}, \mathbf{y}_n + \frac{\Delta t}{2}\mathbf{k}_2\right) \tag{24}$$

$$\mathbf{k}_4 = \mathbf{f}\left(t_n + \Delta t, \mathbf{y}_n + \Delta t\ \mathbf{k}_3\right) \tag{25}$$

These values are then weighted and summed over to achieve the best approximation for the actual derivative. This derivative acts as the slope in a simple linear equation to estimate the next value of $\mathbf{y}$, as can be seen in Eq. 26 [7].

$$\mathbf{y}_{n+1} = \mathbf{y}_n + \frac{\Delta t}{6}\left(\mathbf{k}_1 + 2\mathbf{k}_2 + 2\mathbf{k}_3 + \mathbf{k}_4\right) \tag{26}$$

The implementation of this method in Python is shown below and follows [7].

```
def rk4(f, tlist, y_0, Omega_nk, omega, omega_nk):
    n = y_0.shape[0]
    nr_steps = len(tlist)
    dt = tlist[1] - tlist[0]
    y = np.zeros((n, nr_steps), complex)
    y[:, 0] = y_0
    for i in range(0, nr_steps - 1):
        k1 = f(tlist[i], y[:, i], Omega_nk, omega, omega_nk)
        k2 = f(tlist[i] + 0.5 * dt, y[:, i] + 0.5 * dt * k1,
             Omega_nk, omega, omega_nk)
        k3 = f(tlist[i] + 0.5 * dt, y[:, i] + 0.5 * dt * k2,
             Omega_nk, omega, omega_nk)
        k4 = f(tlist[i] + dt, y[:, i] + dt * k3,
             Omega_nk, omega, omega_nk)
        y[:, i + 1] = y[:, i] + (dt/6.0) * (k1 + 2*k2 + 2*k3 + k4)
    return y
```

Here, the input function `f` represents Eq. 17 and is implemented as a matrix multiplication as follows:

```
import numpy as np
def f(t, y, Omega_nk, omega, omega_nk):
    c = y
```

```
    sum_exp_terms = np.exp(1j * (omega - omega_nk) * t) +
                    np.exp(-1j * (omega + omega_nk) * t)
    M = Omega_nk / 2 * sum_exp_terms
    dc = - 1j * np.matmul(M.T, c)
    return dc
```

The parameters implemented as matrices are

- `Omega_nk` ... the Rabi-frequency Ω_{nk} defined in Eq. 16
- `omega_nk` ... the resonant frequency ω_{nk} defined in Eq. 1
- `omega` ... the frequency ω of the driving field $\mathbf{E}(t)$

In this way, the implementation of the Runge-Kutta method `rk4` uses the function `f` to calculate the derivative for each time step and finally returns the solution matrix $\mathbf{y}$ containing the coefficients c_k for all time steps.

This leaves us with the task of calculating the expectation value of the dipole moment d as defined in Eq. 19 which is realized below.

```
def calculate_dipole_moment(tlist, clist, omega_nk, d_nk):
    c_list_conjugate = np.conj(c_list)
    exp_matrix = np.exp(1j * omega_nk[:, :, np.newaxis] * tlist)
    d_matrix = d_nk[:, :, np.newaxis]
    c_matrix = c_list_conjugate[:, np.newaxis, :] *
               c_list[np.newaxis, :, :]
    d = np.sum(c_matrix * exp_matrix * d_matrix, axis=(0, 1))

    # dipole moment is a real number
    if np.all(np.isclose(d.imag, 0, atol=1e-13)):
        d = d.real
    else:
        print("Warning: d is not real.")
    return d
```

In this implementation `clist` is the output of the Runge-Kutta function `rk4` and `d_nk` is the dipole moment in matrix form. The calculated dipole moment is then returned as an array for all time steps.

4 Validation of numerical solution

To validate the numerical solution discussed in Chapter 3, we seek an analytical solution for Eq. 17 and compare the two solutions. To enable an analytical solution it is necessary to simplify the differential equations by applying the so-called rotating wave approximation. This approximation neglects the term $e^{-i(\omega+\omega_{nk})t}$ since we assumed that $\delta = \omega - \omega_{nk} \ll \omega + \omega_{nk}$ and therefore the term only represents a very fast oscillation with no significant influence on the oscillation between two energy levels [8]. Next, we restrict ourselves to a two-level system, thereby Eq. 17 reduces to the following expression:

$$\dot{c}_1(t) = -i\ c_2(t)\ \frac{\Omega}{2}\ e^{i\delta t} \tag{27}$$

$$\dot{c}_2(t) = -i\ c_1(t)\ \frac{\Omega}{2}\ e^{-i\delta t}. \tag{28}$$

Here, we used the fact that $\Omega_{nk} = \Omega_{kn}$ and $\Omega_{nn} = 0$.

Next, we differentiate Eq. 27 again and substitute $\dot{c_1}$ in Eq. 28 leading to [8]

$$\ddot{c_1}(t) - i\delta\dot{c_1}(t) + \frac{\Omega^2}{4}c_1(t) = 0. \tag{29}$$

This differential equation can now easily be solved using the ansatz $c_1(t) = e^{\lambda t}$ resulting in the general solution

$$c_1(t) = e^{i\frac{\delta}{2}t}\ \left(K_1 e^{i\frac{\Omega_R}{2}t} + K_2 e^{-i\frac{\Omega_R}{2}t}\right), \tag{30}$$

where we have introduced the Rabi flopping frequency defined as follows [8]

$$\Omega_R = \sqrt{\delta^2 + \Omega^2}. \tag{31}$$

Taking the time-derivative of Eq. 30 and substituting it into Eq. 27 yields the general solution for the second coefficient

$$c_2(t) = -\frac{1}{\Omega}e^{-i\frac{\delta}{2}t}\ \left(K_1 e^{i\frac{\Omega_R}{2}t}\ (\delta + \Omega_R) + K_2 e^{-i\frac{\Omega_R}{2}t}\ (\delta - \Omega_R)\right). \tag{32}$$

The specific solutions for the intitial conditions $c_1(0) = 1$ and $c_2(0) = 0$ are then given by

$$c_1(t) = e^{i\frac{\delta}{2}t} \left(\cos\left(\frac{\Omega_R t}{2}\right) - i\frac{\delta}{\Omega_R} \sin\left(\frac{\Omega_R t}{2}\right) \right) \tag{33}$$

$$c_2(t) = -i\frac{\Omega}{\Omega_R} e^{-i\frac{\delta}{2}t} \sin\left(\frac{\Omega_R t}{2}\right). \tag{34}$$

Note that it is straight-forward to calculate the dipole moment from these expressions using Eq. 19. For the actual numerical calculations, we use values obtained for the molecule 4-amino-4'-nitrobiphenyl. These values are taken from [1] and shown in Tables 1 and 2. Note that the values are given in electron volts and Debye but the calculations are performed in atomic units, since the equations were derived using atomic units. The solutions can be found in Figs. 1-3.

Table 1: Parameters of the driving field.
E_0...amplitude of the driving field
ω...frequency of the driving field

E_0 / eV	ω / eV
0.0866	2.17

Table 2: Simulation parameters for the molecule 4-amino-4'-nitrobiphenyl.
d_{nk}...dipole moment between states $|\varphi_n\rangle$ and $|\varphi_k\rangle$
ω_{nk}...resonance frequency between levels E_n and E_k
Ω_{nk}...Rabi frequency between states $|\varphi_n\rangle$ and $|\varphi_k\rangle$
n, k...the row and column index of the matrices

d_{nk} / D	ω_{nk} / eV	Ω_{nk} / eV
$\begin{bmatrix} 0 & 7.76 \\ 7.76 & 0 \end{bmatrix}$	$\begin{bmatrix} 0 & -2.17 \\ 2.17 & 0 \end{bmatrix}$	$\begin{bmatrix} 0 & 0.14 \\ 0.14 & 0 \end{bmatrix}$

As demonstrated in Figs. 1-3, the numerically approximated solution matches the analytical one. The order of magnitude of the error determined using the l_2-norm is 10^{-12}. Also, the numerically exact solution is very close to the other two. The deviation is the result of the term $e^{-i(\omega+\omega_{nk})t}$ that is neglected in the rotating wave approximation but not in the numerically exact solution. This term introduces an added high frequency to the oscillation.

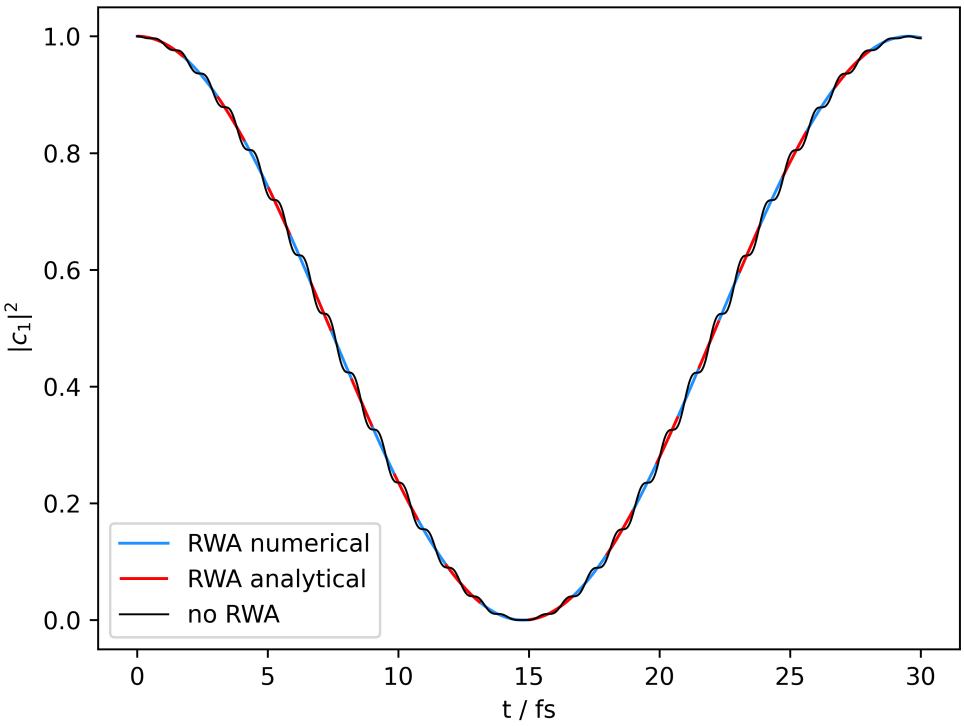

Fig. 1: Ground state occupation as a function of time. Numerical solution without rotating wave approximation (black), numerical solution with rotating wave approximation (blue), analytical solution with rotating wave approximation (red). The parameters used for these calculations can be seen in Tables 1 and 2.

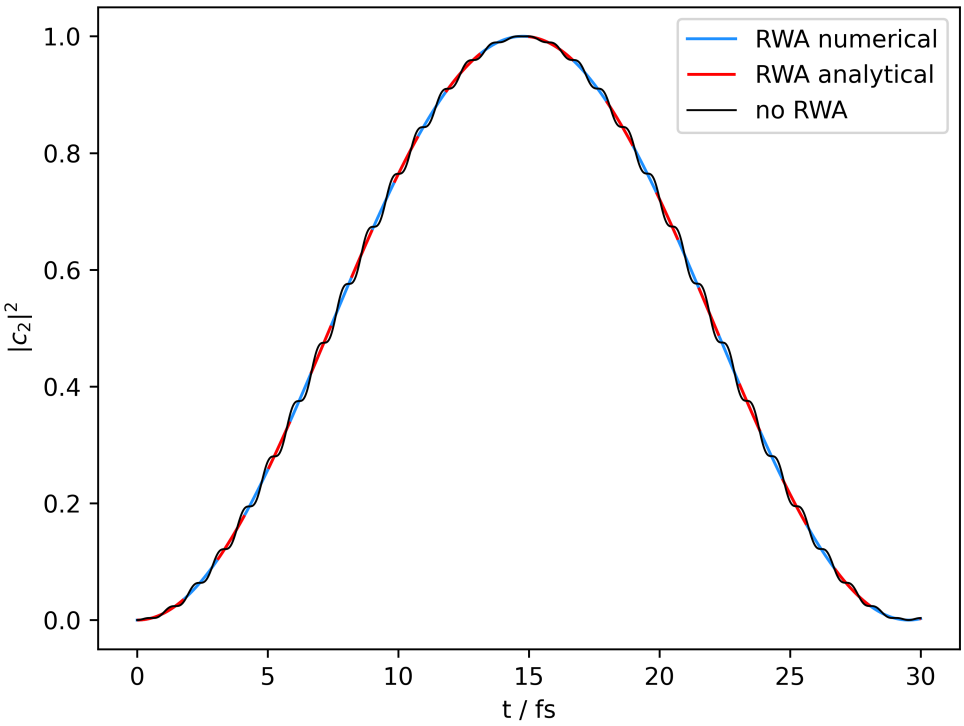

Fig. 2: Excited state occupation as a function of time. Numerical solution without rotating wave approximation (black), numerical solution with rotating wave approximation (blue), analytical solution with rotating wave approximation (red). The parameters used for these calculations can be seen in Tables 1 and 2.

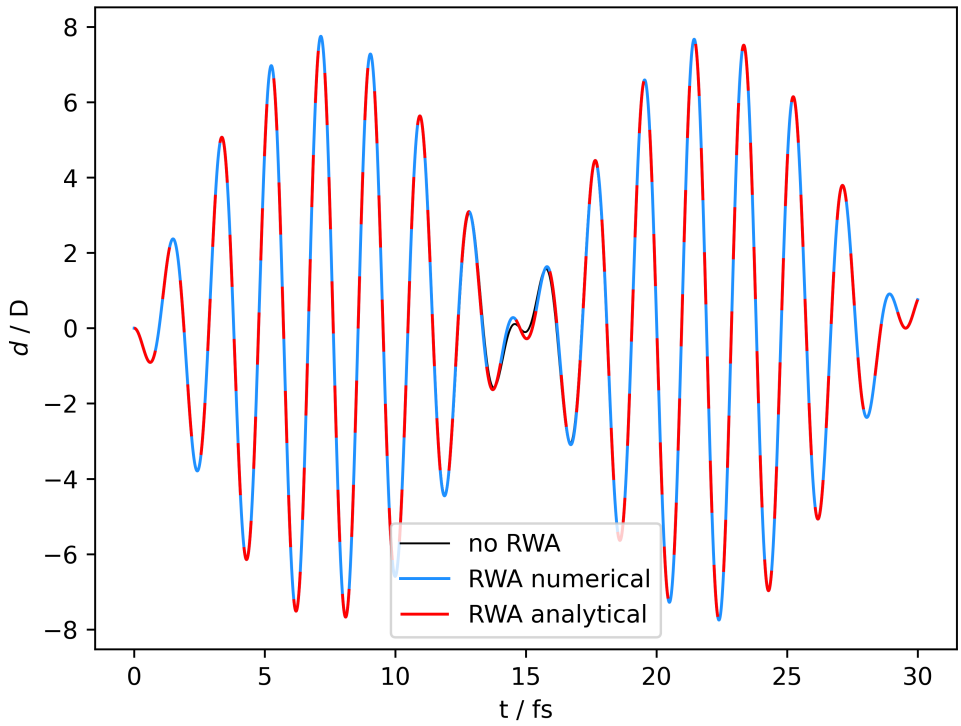

Fig. 3: Dipole moment as a function of time. Numerical solution without rotating wave approximation (black), numerical solution with rotating wave approximation (blue), analytical solution with rotating wave approximation (red). The parameters used for these calculations can be seen in Tables 1 and 2.

5 Results

For the main computations, we consider the molecule NH2-4P-NO2 with the chemical formula $C_{24}H_{18}O_2N_2$ as an example. It is composed of an amino group (NH_2), four phenyl groups and a nitro group (NO_2). For visualization the HOMO (highest occupied molecular orbital) and LUMO (lowest unoccupied molecular orbital) of this molecule are shown in Figs. 4 and 5.

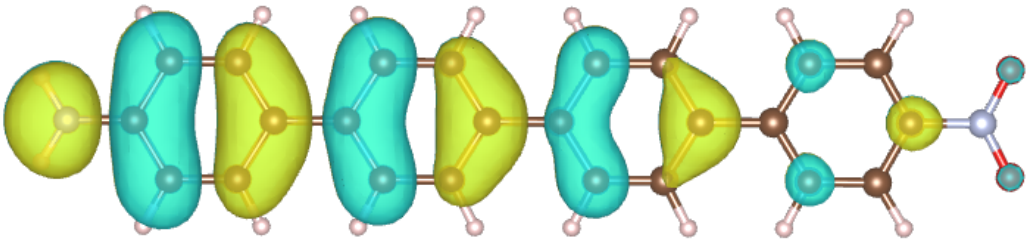

Fig. 4: The HOMO (highest occupied molecular orbital) of NH2-4P-NO2 with the amino group on the left connected to four benzene rings and the nitro group on the right. The simulation is taken from [2] and visualized using the software VESTA 3 [5].

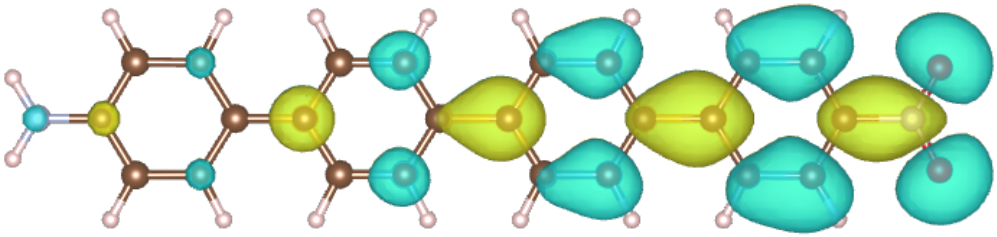

Fig. 5: The LUMO (lowest unoccupied molecular orbital) of NH2-4P-NO2 with the amino group on the left connected to four benzene rings and the nitro group on the right. The simulation is taken from [2] and visualized using the software VESTA 3 [5].

First we consider a two-level-system consisting of the HOMO and LUMO of the molecule NH2-4P-NO2. Later, higher energy levels will be added up to a five-level-system. The parameters of the system for this molecule are taken from [2] and can be found in Table 3. Note that for the computations only the relevant submatrix of the complete matrix is considered. So for a N-level-system, only the $N \times N$ submatrix is used.

The solution of the two-level-system for various detunings $\delta_{21} = \omega - \omega_{21}$ can be seen in Figs. 6a-6c. In Fig. 6a the frequency ω of the driving field matches the resonance fre-

Table 3: Simulation parameters for the molecule NH2-4P-NO2 for a 2- and 3-level-system [2].
d_{nk}...dipole moment between states $|\varphi_n\rangle$ and $|\varphi_k\rangle$
ω_{nk}...resonance frequency between levels E_n and E_k
Ω_{nk}...Rabi frequency between states $|\varphi_n\rangle$ and $|\varphi_k\rangle$
n, k...the row and column index of the matrices

d_{nk} / D
$\begin{bmatrix} 0.00 & -6.28 & 6.53 \\ -6.28 & 0.00 & -15.08 \\ 6.53 & -15.08 & 0.00 \end{bmatrix}$

ω_{nk} / eV
$\begin{bmatrix} 0.00 & -2.69 & -3.79 \\ 2.69 & 0.00 & -1.10 \\ 3.79 & 1.10 & 0.00 \end{bmatrix}$

Ω_{nk} / eV
$\begin{bmatrix} 0.00 & -0.11 & 0.12 \\ -0.11 & 0.00 & -0.27 \\ 0.12 & -0.27 & 0.00 \end{bmatrix}$

quency ω_{21} exactly, resulting in the maximum possible oscillation. When the frequency is slightly off as in Fig. 6b, the excited state is never fully occupied and the ground state never empty. In Fig. 6c the driving field frequency is far away from the resonant frequency. The ground state is almost fully occupied and the excited state almost empty with only slight oscillations.

What can be observed in Fig. 6a is that in the resonant case the frequency of the dipole moments envelope is the same as the frequency at which the occupation of the states oscillates. When moving away from resonance, the dipole moments envelope broadens and eventually develops a new node between the previous nodes. This intermediate state is depicted in Fig. 6b. The newly developed nodes half the period of the envelope, which can be observed in Fig. 6c [1].

Next, we will look at systems with more than two levels going up to a five-level-system. The solutions for those systems are shown in Figs. 7a-9b. In Figs. 7a and 7c one can see the maximum possible excitation of the second and third level if the frequency of the driving field matches the respective resonance frequency. Fig. 7b shows that if the driving field frequency is the mean of the resonance frequencies ω_{21} and ω_{31}, both levels are approximately equally excited.

Table 4: Simulation parameters for the molecule NH2-4P-NO2 for a 4- and 5-level-system with $E_0 = 0.0866$ V/Å and modified dipole moment [2].
d_{nk}...dipole moment between states $|\varphi_n\rangle$ and $|\varphi_k\rangle$
ω_{nk}...resonance frequency between levels E_n and E_k
Ω_{nk}...Rabi frequency between states $|\varphi_n\rangle$ and $|\varphi_k\rangle$
n, k...the row and column index of the matrices

d_{nk} / D

$$\begin{bmatrix} 0.00 & -6.28 & 6.53 & 2.54 & 2.54 \\ -6.28 & 0.00 & -15.08 & 0.00 & 0.00 \\ 6.53 & -15.08 & 0.00 & 0.00 & 0.00 \\ 2.54 & 0.00 & 0.00 & 0.00 & -12.60 \\ 2.54 & 0.00 & 0.00 & -12.60 & 0.00 \end{bmatrix}$$

ω_{nk} / eV

$$\begin{bmatrix} 0.00 & -2.69 & -3.79 & -4.41 & -4.78 \\ 2.69 & 0.00 & -1.10 & -1.72 & -2.09 \\ 3.79 & 1.10 & 0.00 & -0.62 & -1.00 \\ 4.41 & 1.72 & 0.62 & 0.00 & -0.38 \\ 4.78 & 2.09 & 1.00 & 0.38 & 0.00 \end{bmatrix}$$

Ω_{nk} / eV

$$\begin{bmatrix} 0.00 & -0.11 & 0.12 & 0.05 & 0.05 \\ -0.11 & 0.00 & -0.27 & 0.00 & 0.00 \\ 0.12 & -0.27 & 0.00 & 0.00 & 0.00 \\ 0.05 & 0.00 & 0.00 & 0.00 & -0.23 \\ 0.05 & 0.00 & 0.00 & -0.23 & 0.00 \end{bmatrix}$$

For the 4- and 5-level-system the probabilities for the transition to level 4 and 5 are zero. So, to achieve excitation in level 4 and 5, the dipole moments d_{14} and d_{15} have to be set to non-zero artificially. Here, we choose $d_{14} = d_{41} = d_{15} = d_{51} = 1\ e \cdot a_0 \approx 2.54$ D. This can be seen from the results shown in Figs. 8a and 8b, where the driving field oscillates at a frequency that is not near the resonant frequency ω_{41}. At a driving field amplitude of $E_0 = 0.0866$ V/Å the system behaves as expected for the given frequency, as can be seen in Fig. 8a. However, if the driving field is much stronger, an excitation in level 4 is possible even outside the resonant frequency. This can be observed in Fig. 8b, where the amplitude is five times the amplitude in Fig. 8a. The same phenomenon is illustrated in Figs. 9a and 9b for a 5-level-system.

Table 5: Simulation parameters for the molecule NH2-4P-NO2 for a 4- and 5-level-system with $E_0 = 0.4332$ V/Å and modified dipole moment [2].
d_{nk}...dipole moment between states $|\varphi_n\rangle$ and $|\varphi_k\rangle$
ω_{nk}...resonance frequency between levels E_n and E_k
Ω_{nk}...Rabi frequency between states $|\varphi_n\rangle$ and $|\varphi_k\rangle$
n, k...the row and column index of the matrices

d_{nk} / D

$$\begin{bmatrix} 0.00 & -6.28 & 6.53 & 2.54 & 2.54 \\ -6.28 & 0.00 & -15.08 & 0.00 & 0.00 \\ 6.53 & -15.08 & 0.00 & 0.00 & 0.00 \\ 2.54 & 0.00 & 0.00 & 0.00 & -12.60 \\ 2.54 & 0.00 & 0.00 & -12.60 & 0.00 \end{bmatrix}$$

ω_{nk} / eV

$$\begin{bmatrix} 0.00 & -2.69 & -3.79 & -4.41 & -4.78 \\ 2.69 & 0.00 & -1.10 & -1.72 & -2.09 \\ 3.79 & 1.10 & 0.00 & -0.62 & -1.00 \\ 4.41 & 1.72 & 0.62 & 0.00 & -0.38 \\ 4.78 & 2.09 & 1.00 & 0.38 & 0.00 \end{bmatrix}$$

Ω_{nk} / eV

$$\begin{bmatrix} 0.00 & -0.57 & 0.59 & 0.23 & 0.23 \\ -0.57 & 0.00 & -1.36 & 0.00 & 0.00 \\ 0.59 & -1.36 & 0.00 & 0.00 & 0.00 \\ 0.23 & 0.00 & 0.00 & 0.00 & -1.14 \\ 0.23 & 0.00 & 0.00 & -1.14 & 0.00 \end{bmatrix}$$

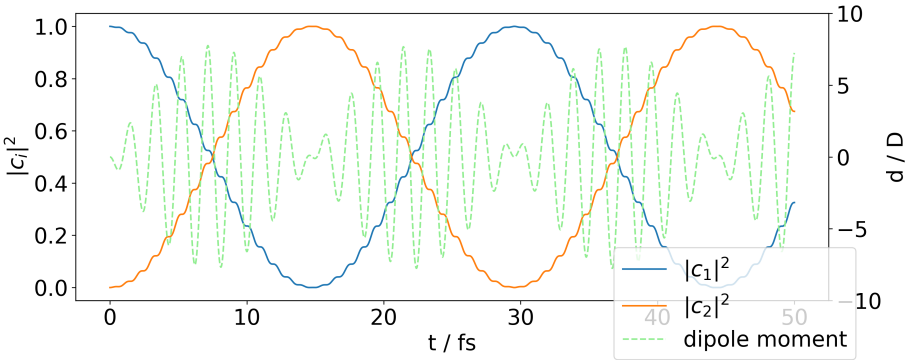

(a) $\delta_{21} = 0.00$ eV, $\omega = 2.689$ eV

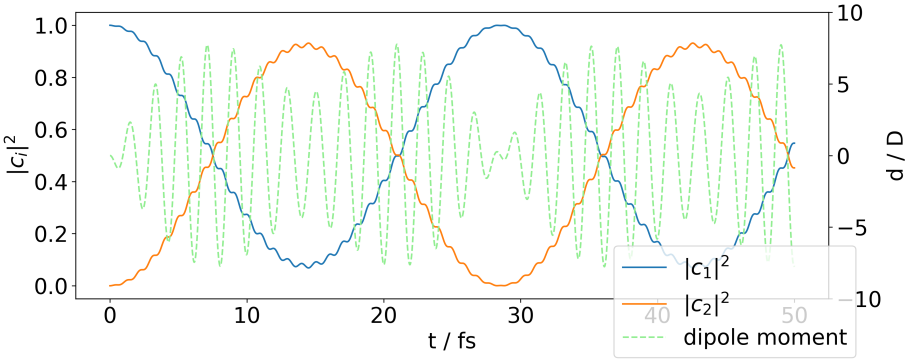

(b) $\delta_{21} = 0.04$ eV, $\omega = 2.729$ eV

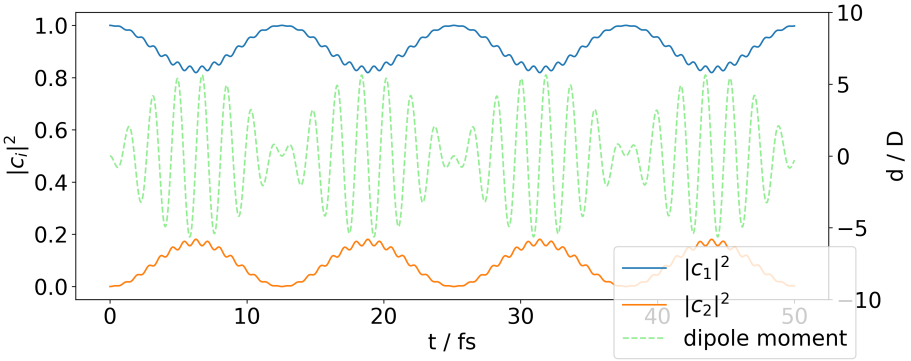

(c) $\delta_{21} = 0.30$ eV, $\omega = 2.989$ eV

Fig. 6: Rabi oscillations of a two-level-system with ground state occupation, excited state occupation and dipole moment as a function of time. The simulation parameters used for the calculation can be found in Table 3. The amplitude of the driving field is $E_0 = 0.0866$ V/Å.

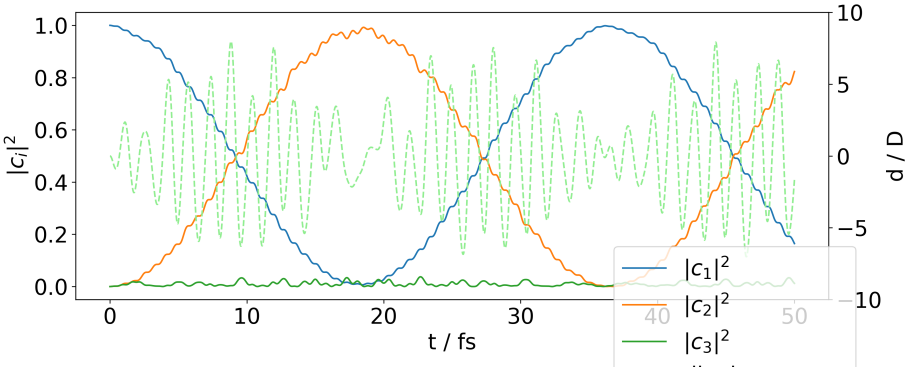

(a) $\omega = \omega_{21} = 2.69$ eV

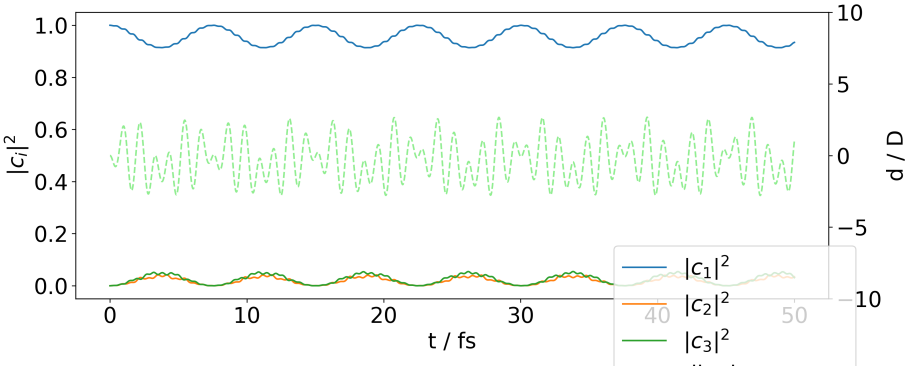

(b) $\omega = \frac{(\omega_{21}+\omega_{31})}{2} = 3.24$ eV

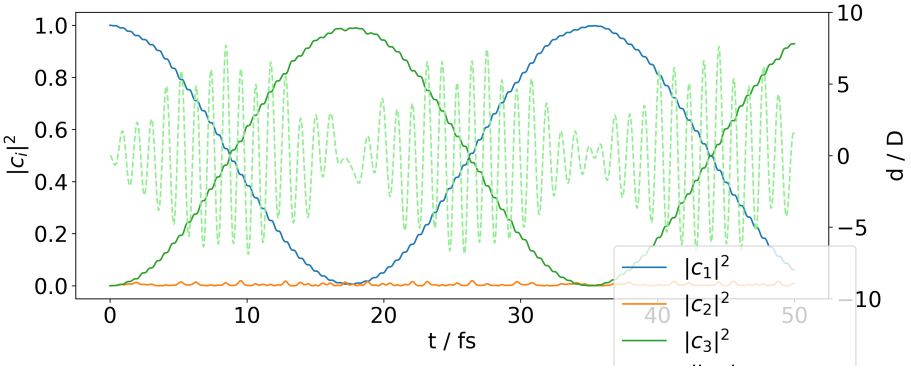

(c) $\omega = \omega_{31} = 3.79$ eV

Fig. 7: Rabi oscillations of a 3-level-system with ground state, first two excited states and dipole moment as a function of time. The simulation parameters used for the calculation can be found in Table 3. The amplitude of the driving field is E_0 = 0.0866 V/Å.

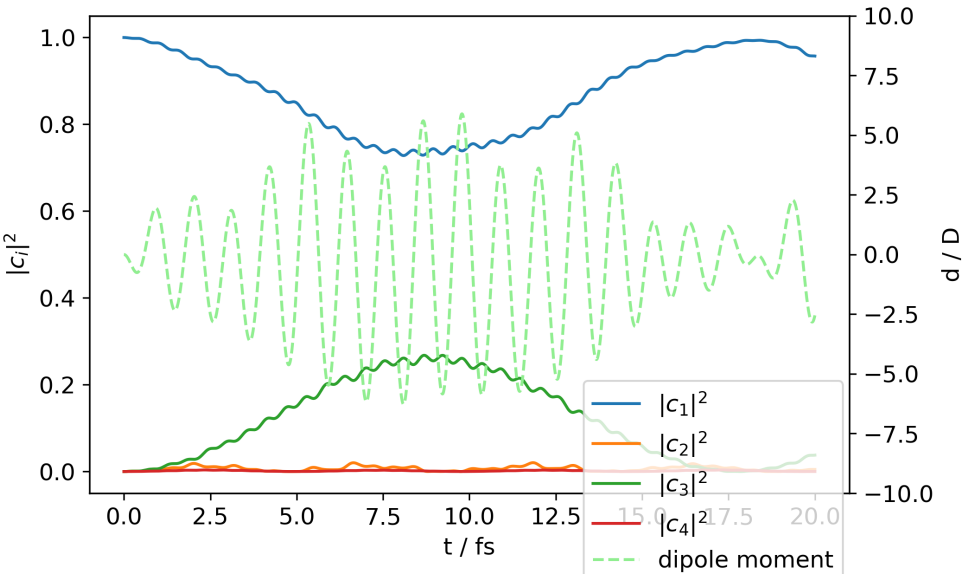

(a) $E_0 = 0.0866$ V/Å

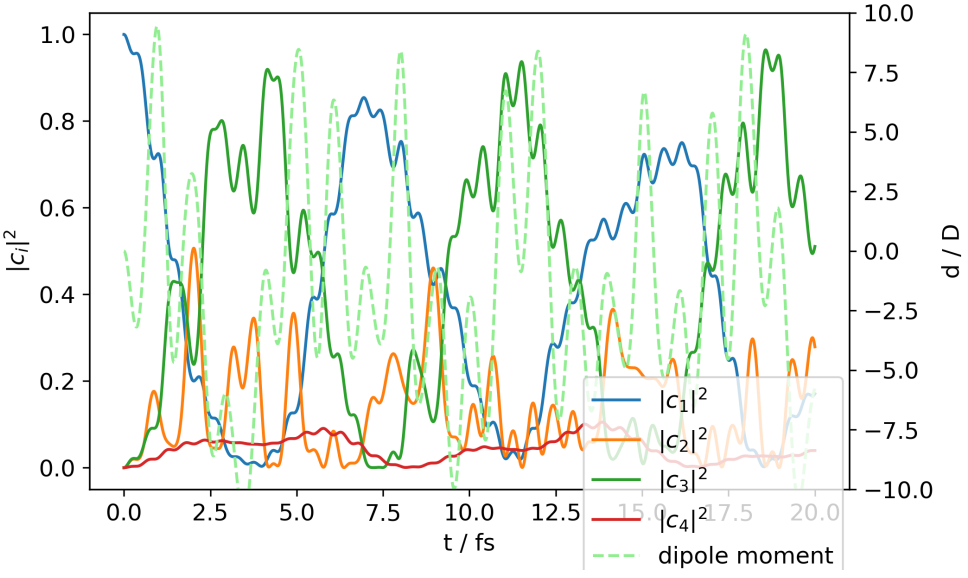

(b) $E_0 = 0.4332$ V/Å

Fig. 8: Rabi oscillations of a 4-level-system with ground state, first three excited states and dipole moment as a function of time. The simulation parameters used for the calculation for (a) can be found in Table 4, for (b) in Table 5. The frequency of the driving field is $\omega = 3.58$ eV.

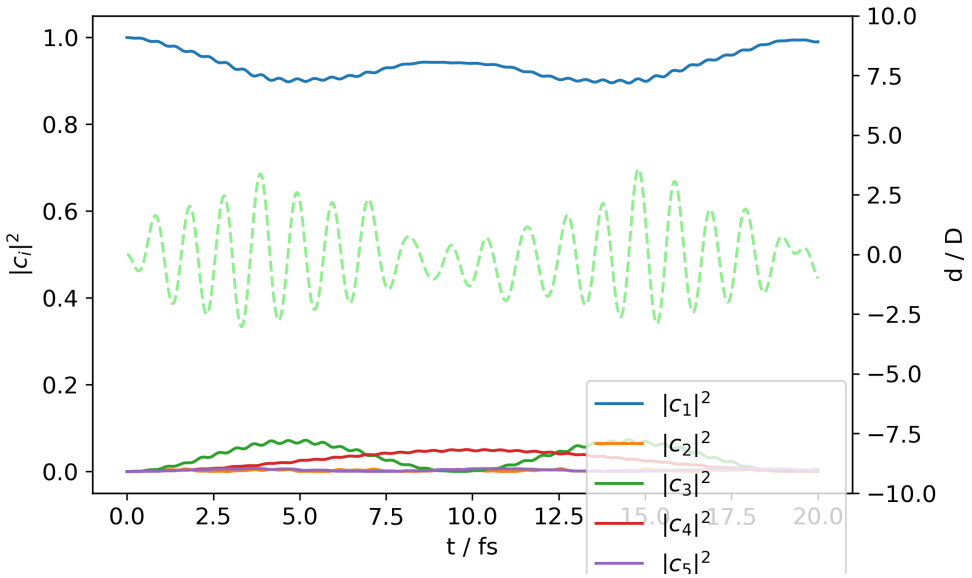

(a) $E_0 = 0.0866$ V/Å

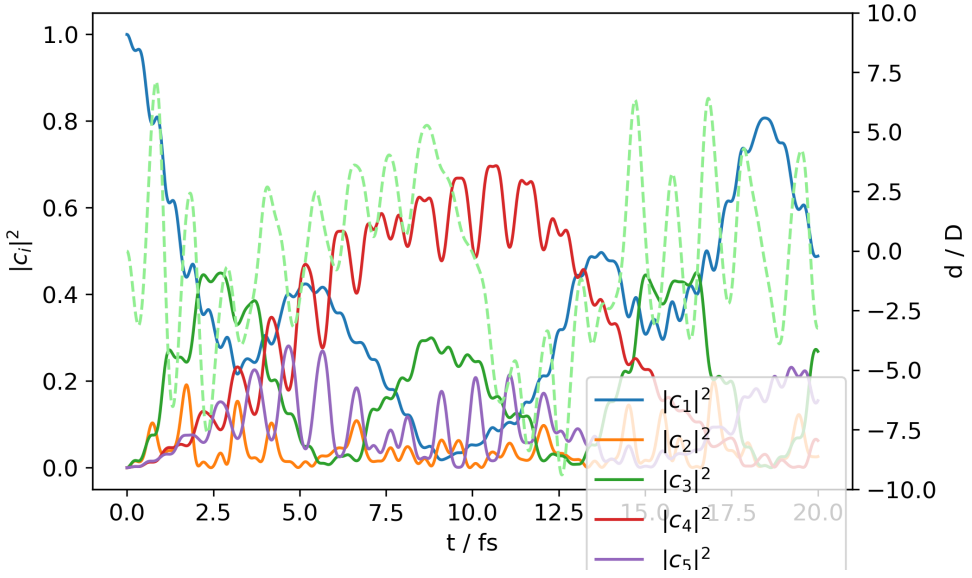

(b) $E_0 = 0.4332$ V/Å

Fig. 9: Rabi oscillations of a 5-level-system with ground state, first four excited states and dipole moment as a function time. The simulation parameters used for the calculation for (a) can be found in Table 4, for (b) in Table 5. The frequency of the driving field is $\omega = 4.20$ eV.

6 Summary

The focus of this work is to numerically predict the time evolution of the occupations in a N-level-system that is driven by a periodic external electric field. The derivation of the problem in Chapter 2 leads to the differential equations in Eq. 17. Furthermore a formula for the dipole moment is derived (Eq. 19). The numerical solution using the Runge-Kutta-method is explained in Chapter 3 and then validated in Chapter 4. This validation involves solving the differential equations for a two-level-system analytically using the rotating wave approximation. This solution is then compared to the numerical solution with the same approximation. The comparison can be seen in Figs. 1-3, demonstrating the numerical error to be indeed very small, thereby indicating that the numerical solution can be trusted. The results are shown in Figs. 6-9 starting with a 2-level-system and ending at a 5-level-system. They show the occupation of the levels together with the systems dipole moment over time.

References

[1] Dominik Brandstetter. Photoemission distributions from time-dependent density functional theory. Karl-Franzens-Universität Graz, 2022.

[2] Dominik Brandstetter, Xiaosheng Yang, Daniel Lüftner, F. Stefan Tautz, and Peter Puschnig. kmap.py: A python program for simulation and data analysis in photoemission tomography. *Computer Physics Communications*, 263:107905, 2021.

[3] David J Griffiths and Darrell F Schroeter. *Introduction to quantum mechanics*. Cambridge university press, 2018.

[4] Ulrich Hohenester. *Nano and Quantum Optics*. Springer, 2020.

[5] Koichi Momma and Fujio Izumi. *VESTA3* for three-dimensional visualization of crystal, volumetric and morphology data. *Journal of Applied Crystallography*, 44(6):1272–1276, Dec 2011.

[6] Makoto Morinaga. Deriving the static interaction between electric dipoles via the quantum gauge transformation. *arXiv:1302.0920*, 2013.

[7] Peter Puschnig. Computerorientierte Physik, 2019. Lecture notes, Karl-Franzens-Universität Graz.

[8] Peter Van der Straten and Harold Metcalf. *Atoms and molecules interacting with light: Atomic physics for the laser era*. Cambridge University Press, 2016.